

Supplementary Materials for
A sustainable single-component “Silk nacre”

Zongpu Xu, Mingrui Wu, Weiwei Gao, Hao Bai*

*Corresponding author. Email: hbai@zju.edu.cn

Published 13 May 2022, *Sci. Adv.* **8**, eabo0946 (2022)
DOI: [10.1126/sciadv.abo0946](https://doi.org/10.1126/sciadv.abo0946)

The PDF file includes:

Figs. S1 to S8
Legend for movie S1

Other Supplementary Material for this manuscript includes the following:

Movie S1

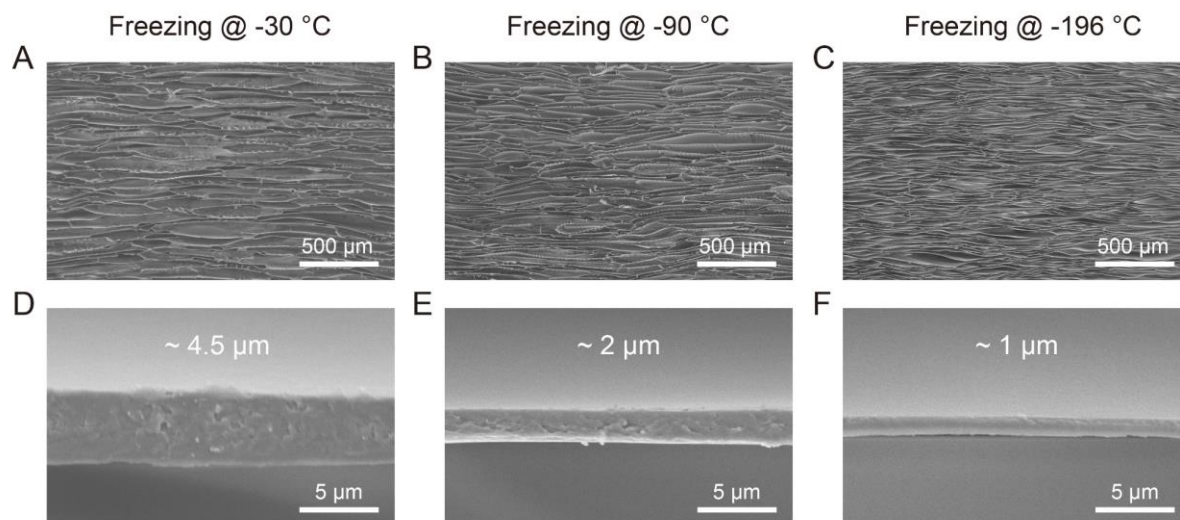


Fig. S1. SEM images of the cross sections of silk aerogels prepared at different cooling temperatures by keeping the copper finger at -30 °C, -90 °C, and -196 °C. (A to C) The cross sections of all samples show long-range aligned lamellar structures. (D to F) Magnified images show that the thicknesses of silk laminae decrease with the reduction in temperature.

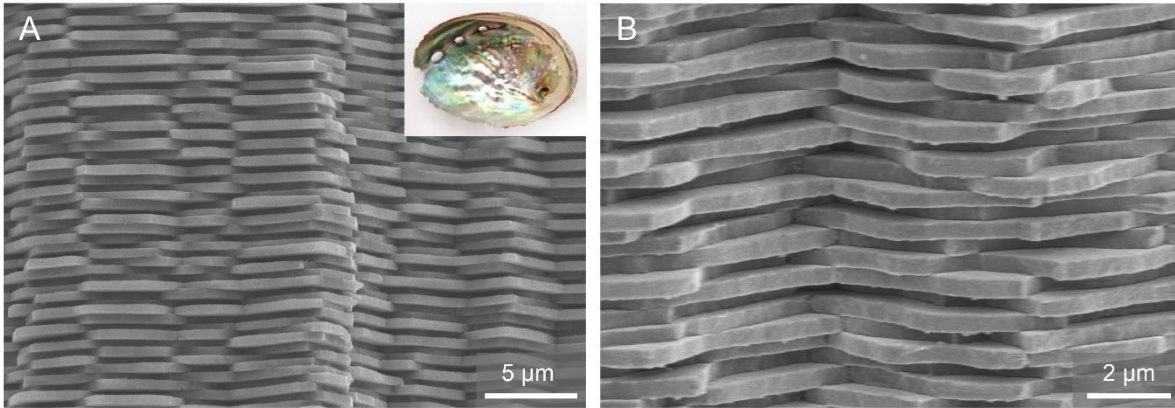


Fig. S2. The morphology and microstructure of natural nacre. (A) SEM image of the cross section of natural nacre and inset is an optical photograph of the nacre formed by an abalone *Haliotis discus hannai*. (B) The magnified SEM image shows nacre's typical lamellar structures.

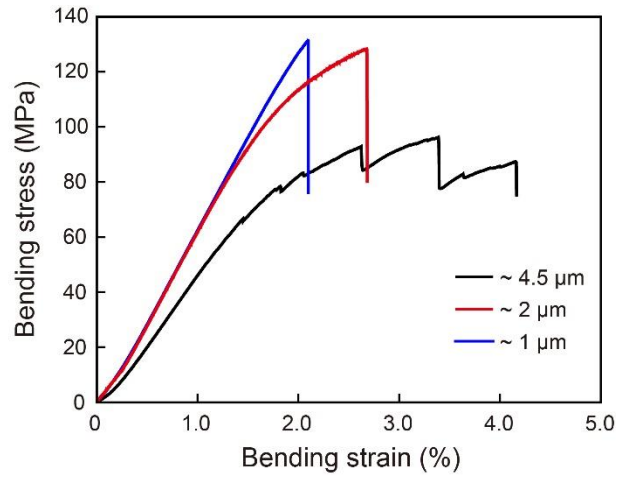


Fig. S3. Stress-strain curves of the “Silk nacre” with different thickness of the laminae. The breaking strength of the “Silk nacre” decreased with the increasing thickness of the silk laminae.

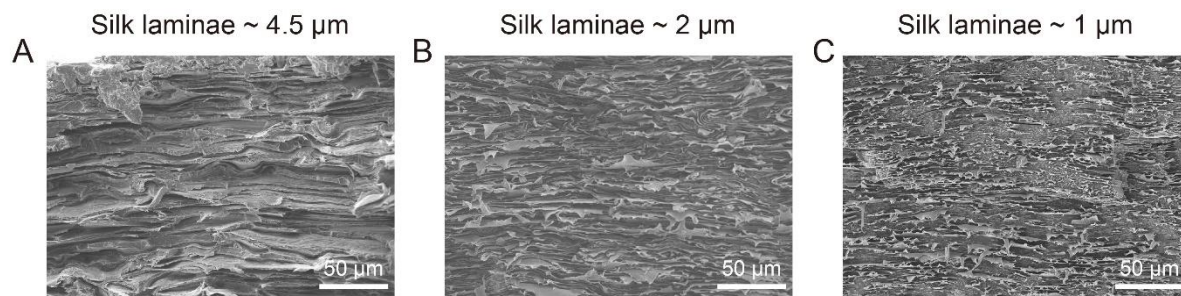


Fig. S4. SEM images showing the fracture cross-sections of the “Silk nacre” with different thickness of the laminae. (A-C) The thickness of silk laminae is ~ 4.5 μm, ~ 2 μm, and ~ 1 μm, respectively.

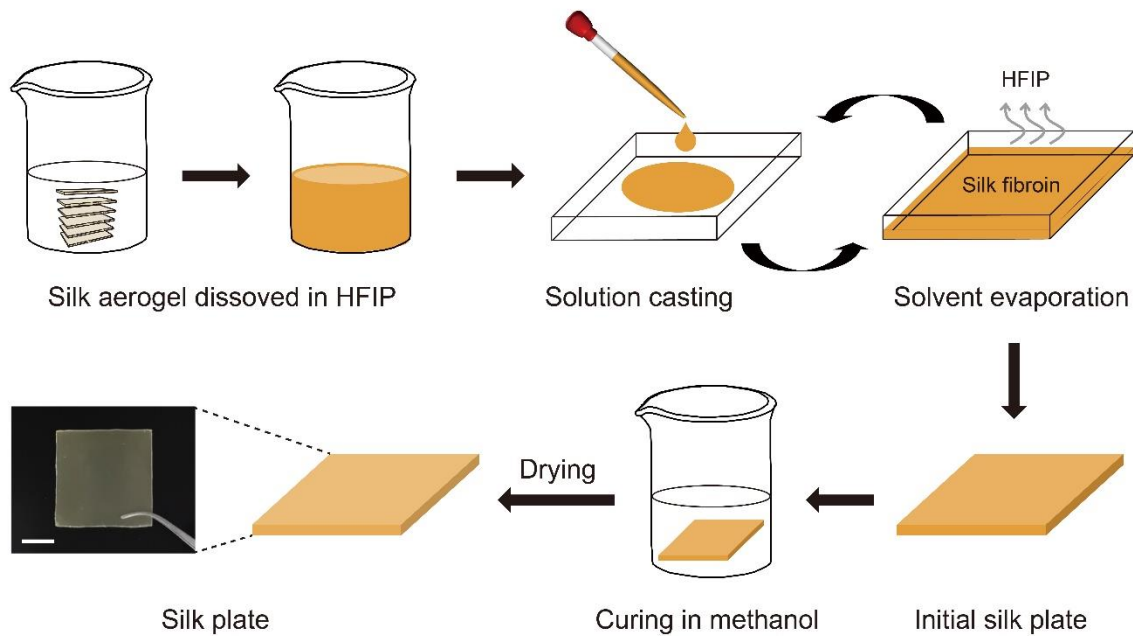


Fig. S5. Schematic diagram of the preparation procedure of homogeneous silk plate. The processes include dissolution of silk aerogel in HFIP, alternate silk-HFIP solution casting and solvent evaporation of HFIP, as well as curing in methanol and drying. The optical photograph shows the as-prepared silk plate, and the scale bar is 1 cm.

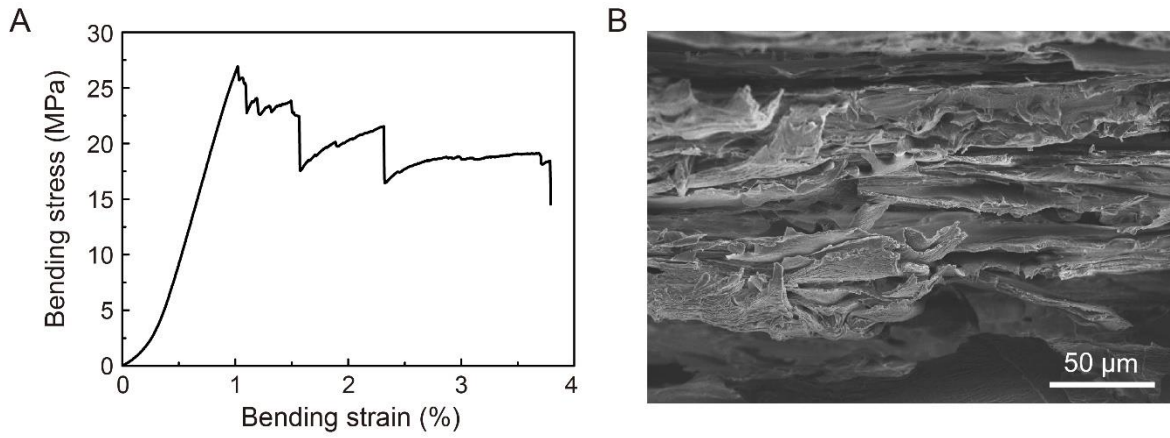


Fig. S6. The mechanical property and fracture morphology of the “Silk nacre” with weak interfaces. (A) Stress-strain curve; (B) SEM image of the fracture surface. This material is prepared by directly pressing the freeze-dried silk aerogel without water vapor annealing.

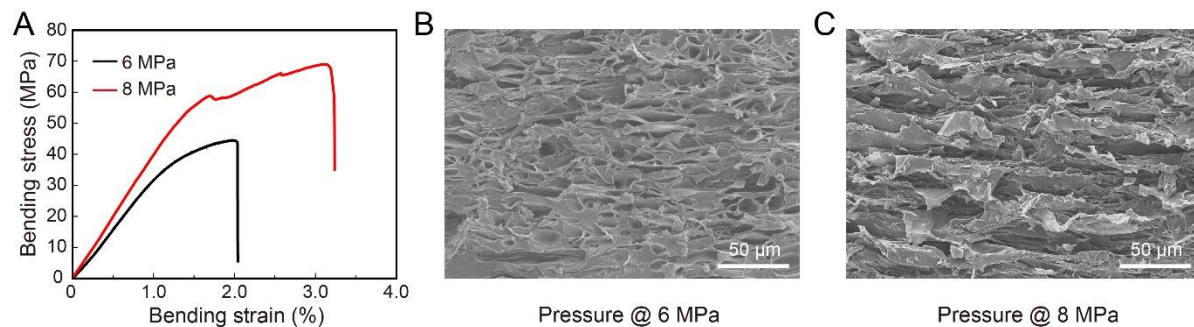


Fig. S7. The mechanical property and fracture morphology of the “Silk nacre” prepared at various compressive pressures. (A) Stress-strain curve; (B, C) The SEM image of the fracture surfaces show the reduction in structural densification as the interlamellar voids are observed.

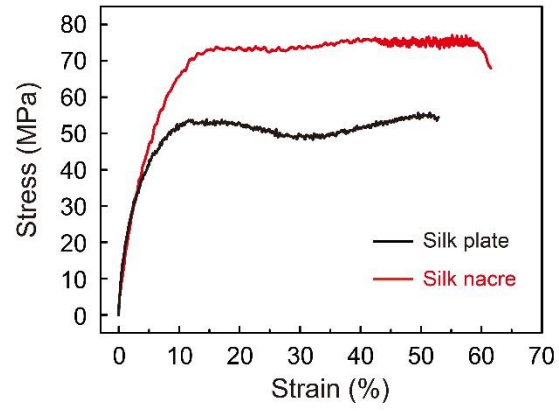


Fig. S8. Stress-strain curves from split Hopkinson pressure bar (SHPB) tests indicate the better impact resistance of the “Silk nacre” than silk plate at high compression strain rate ($10,000 \text{ s}^{-1}$).

Movie S1. The falling ball impact tests show the better impact resistance of the “Silk nacre” than silk plate.